Dynamics of a mesoscopic charge quantum bit under continuous quantum measurement

Hsi-Sheng Goan* and Gerard J. Milburn
Center for Quantum Computer Technology and Department of Physics, University of Queensland, Brisbane, Queensland 4072, Australia
(Received 1 March 2001; revised manuscript received 6 July 2001; published 16 November 2001)

We present the conditional quantum dynamics of an electron tunneling between two quantum dots subject to a measurement using a low transparency point contact or tunnel junction. The double dot system forms a single qubit and the measurement corresponds to a continuous in time readout of the occupancy of the quantum dot. We illustrate the difference between conditional and unconditional dynamics of the qubit. The conditional dynamics is discussed in two regimes depending on the rate of tunneling through the point contact: quantum jumps, in which individual electron tunneling current events can be distinguished, and a diffusive dynamics in which individual events are ignored, and the time-averaged current is considered as a continuous diffusive variable. We include the effect of inefficient measurement and the influence of the relative phase between the two tunneling amplitudes of the double dot/point contact system.

DOI: 10.1103/PhysRevB.64.235307 PACS number(s): 73.63.Kv, 85.35.Be, 03.65.Ta, 03.67.Lx

I. INTRODUCTION

One of the key requirements for a physically implementing a quantum computational scheme is the ability to readout a single quantum bit (qubit) with high efficiency.[1] In an ion trap implementation this problem has already been solved using shelving spectroscopy.[2] However in solid state schemes implementing a high efficiency measurement of the charge or spin degree of freedom of a single electron (or Cooper pair) will be very challenging. Various implementations of quantum bits (qubits) and quantum gates for a solid-state quantum computer has been proposed.[3–7] The conditional dynamics of a single quantum particle (qubit) in a single realization of continuous measurements is quite different from the ensemble average (unconditional) behavior that is more familiar to the condensed matter physics community. An apparatus by its very nature as a measurement device, must at least cause decoherence of the measured system in the basis which diagonalizes the measured quantity. From this perspective, the measurement apparatus behaves like an environment, that is, a system with many degrees of freedom for which correlations between its subcomponents decay rapidly with time. Indeed for a system to function as a measurement apparatus it must be composed of many degrees of freedom.[8] Thus every measured system is an open system. To understand the influence of the detector (environment) on the measured system, the conventional approach is to study the (unconditional) master equation of the reduced density matrix. However, integrating or tracing out the environmental (detector) degrees of the freedom to obtain the reduced density matrix is equivalent to completely ignoring or averaging over the results of all measurement records. This averaging means the detector is treated as a pure environment for the system, rather than a measurement device which can provide information about the change of the state of the qubit. On the other hand, for the purpose of quantum computing, it is important to understand how the quantum state of a single qubit, conditioned on a particular single realization of the measurement, evolves in time. A number of questions need to be answered that cannot be answered if we only determine the ensemble averaged behavior of the measured qubit. For example, in the case of a continuous measurement it is necessary to determine how long it takes for a confident determination of the state of the qubit at the start of the measurement, even if the qubit itself undergoes additional coherent evolution during the measurement process. Furthermore it may be possible to consider adaptive measurement schemes which take a given time continuous measurement record, subject it to real-time signal processing, and then change the way in which the measurement acts through a feedback loop. Such schemes are already being implemented in quantum optics and offer the promise of reaching sensitivities at the quantum limit.[9,10]

We illustrate, in this paper, the difference between conditional and unconditional (ensemble average) dynamics by considering the problem of an electron tunneling between two coherently coupled quantum dots (CQD's), a two-state quantum system (qubit), using a low-transparency point contact (PC) or tunnel junction as a detector (environment) continuously measuring the position of the electron, schematically illustrated in Fig. 1. We assume strong inner and inter

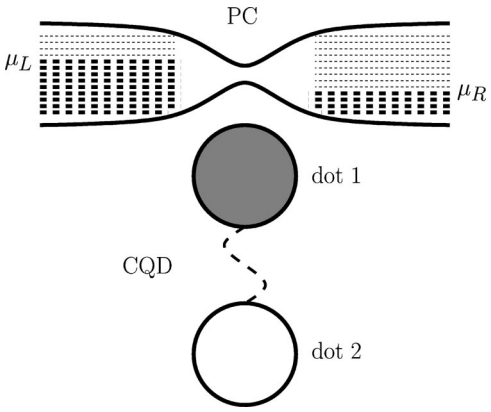

FIG. 1. Schematic representation of an electron tunneling between two coupled quantum dots (CQD's), a two-state quantum system (qubit), using a low-transparency point contact (PC) or tunnel junction as a detector (environment) continuously measuring the position of the electron. Here μ_L and μ_R stand for the chemical potentials in the left and right reservoirs, respectively.

dot Coulomb repulsion, so only one electron can occupy this CQD system. The logical qubit states in this case are, respectively, the perfect localization of the electron charge states in one of the two CQD's. A controlled-not-gate operation based on the charge qubit of two asymmetric CQD's has been suggested in Ref. 7. Experimentally, coherent coupling between two CQD's has been reported. It has been shown[11,12] that if the inter-dot tunneling barrier is low and the strength of the coupling of two CQD's is strong, the two CQD's behave as a large single dot in a Coulomb blockade phenomenon. In addition, the energy splitting between bonding and antibonding states of two CQD's has been confirmed by microwave absorption measurements.[13,14] The CQD system studied here is similar to the superconducting Cooper-pair-box charge qubit[5,15,16] in that they both use charge degrees of freedom as qubit basis states. For the superconducting Cooper-pair box, the charge on the island differs by the number of Cooper pairs times the charge $2e$, compared to the electron charge e in one of the two dots in the CQD system. The PC, considered here, is a charge-sensitive detector. The tunneling barrier height or the current through the tunneling junction of the PC detector depends on the proximity of an external charge. Hence the study of charge measurements by a PC detector is applicable to different types of charge qubit, such as the CQD's or the Cooper-pair box. The problem of the CQD system measured by a low-transparency PC has been extensively studied in Refs. 17–26. The case of measurements by a general quantum point contact detector with arbitrary transparency has also been investigated in Refs. 27–32. In addition, a similar system, a Cooper-pair-box qubit, measured by a single electron transistor has been studied in Refs. 33, 22, 20, 23, 25, 34, and 35.

Korotkov[19,21,25] has obtained the Langevin rate equations for the CQD system measured by an ideal PC detector. These rate equations describe the random evolution of the density matrix that both conditions, and is conditioned by, the PC detector output. Recently, Ref. 26 presented a *quantum trajectory*[36–46] measurement analysis of the same system. We found that the conditional dynamics of the CQD system can be described by the stochastic Schrödinger equation for the conditioned state vector, provided that the information carried away from the CQD system by the PC reservoirs can be recovered by the perfect detection of the measurements. We also analyzed the localization rates at which the qubit becomes localized in one of the two states when the coupling frequency Ω between the states is zero. We showed that the localization time discussed there is slightly different from the measurement time defined in Refs. 33,22,23. The mixing rate at which the two possible states of the qubit become mixed when $\Omega \neq 0$ was calculated as well and found in agreement with the result in Refs. 22 and 23. In this paper, we focus on the qubit dynamics conditioned on a particular realization of the actual measured current through the PC device. Especially, we take into account the effect of inefficient measurement on the conditional dynamics and illustrate the conditional quantum evolutions by numerical simulations.

The problem of a ''nonideal'' detector was discussed in Refs. 19–21. There the nonideality of the detector is modeled as two ideal detectors ''in parallel'' with the output of the second detector inaccessible. The information loss is due to the interaction with the second detector, treated as a ''pure environment'' (which does not affect the observed detector current). As a consequence, the decoherence rate, $\Gamma_{\rm tot}$, in that case is larger than the decoherence rate for the PC as an environment alone, $\Gamma_{\rm tot}-\Gamma_d=\gamma_d>0$. Hence an extra decoherence term, $-\gamma_d\rho_{ab}$, for example, is added in the rate equation $\dot{\rho}_{ab}$. However, this approach does not account for the inefficiency in the measurements, which arises when the detector sometimes misses detection. In that case, there is still only one PC detector (environment) and disregarding all measurement records leads to $\Gamma_{\rm tot}=\Gamma_d$. Furthermore, the detector current is affected and in fact reduced by the inefficiency in the measurements.

In this paper, we take into account the effect of inefficient measurement of the PC detector on the dynamics of the qubit. We also analyze the conditional qubit dynamics analytically and numerically. The different behavior of unconditional and conditional evolution is demonstrated. We present the conditional quantum dynamics over the full range of behavior, from quantum jumps to quantum diffusion.[26] In Refs. 17, 19, 21, and 25, the two tunneling amplitudes of the CQD–PC model were assumed to be real. In Ref. 26, the relative phase between them was taken into account. Here, we discuss and illustrate furthermore their influence on the qubit dynamics. In Sec. II, we describe the model Hamiltonian and the unconditional master equation. We then obtain in Sec. III the quantum-jump and quantum-diffusive, conditional master equations for the case of inefficient measurements. Section IV is devoted to the analysis for the qubit dynamics. Numerical simulations of the conditional evolution are presented in this section. Finally, a short conclusion is given in Sec. V. In the Appendix, the stationary noise power spectrum of the current fluctuations through the PC barrier is calculated in terms of the quantum-jump formalism.

II. UNCONDITIONAL MASTER EQUATION FOR THE CQD AND PC MODEL

Following the model of Refs. 17, 19, 21, and 26, we describe the whole system (see Fig. 1) by the following Hamiltonian:

$$\mathcal{H}=\mathcal{H}_{\rm CQD}+\mathcal{H}_{\rm PC}+\mathcal{H}_{\rm coup}, \tag{1}$$

where

$$\mathcal{H}_{\rm CQD}=\hbar[\omega_1 c_1^\dagger c_1+\omega_2 c_2^\dagger c_2+\Omega(c_1^\dagger c_2+c_2^\dagger c_1)], \tag{2}$$

$$\mathcal{H}_{\rm PC}=\hbar\sum_k\,(\omega_k^L a_{Lk}^\dagger a_{Lk}+\omega_k^R a_{Rk}^\dagger a_{Rk}) +\sum_{k,q}\,(T_{kq}a_{Lk}^\dagger a_{Rq}+T_{qk}^* a_{Rq}^\dagger a_{Lk}), \tag{3}$$

$$\mathcal{H}_{\rm coup}=\sum_{k,q}\,c_1^\dagger c_1(\chi_{kq}a_{Lk}^\dagger a_{Rq}+\chi_{qk}^* a_{Rq}^\dagger a_{Lk}). \tag{4}$$

$\mathcal{H}_{\rm CQD}$ represents the effective tunneling Hamiltonian for the measured CQD system (mesoscopic charge qubit). The tunneling Hamiltonian for the PC detector is represented by $\mathcal{H}_{\rm PC}$. Here c_i ($c_i^\dagger$) and $\hbar\omega_i$ represent the electron annihilation (creation) operator and energy for a single electron state in each dot, respectively. The coupling between these two dots is given by $\hbar\Omega$. Similarly, a_{Lk}, a_{Rk} and $\hbar\omega_k^L, \hbar\omega_k^R$ are, respectively, the electron annihilation operators and energies for the left and right reservoir states at wave number k. $\mathcal{H}_{\rm coup}$, Eq. (4), describes the interaction between the detector and the measured system, depending on which dot is occupied. When the electron in the CQD system is located in dot 1, the effective tunneling amplitude of the PC detector changes from $T_{kq} \to T_{kq} + \chi_{kq}$.

The (unconditional) zero-temperature,[47] Markovian master equation of the reduced density matrix for the CQD system (qubit) has been obtained in Refs. 17 and 26:

$$\dot{\rho}(t) = -\frac{i}{\hbar}[\mathcal{H}_{\rm CQD}, \rho(t)] + \mathcal{D}[\mathcal{T} + \mathcal{X} n_1]\rho(t) \tag{5a}$$

$$\equiv \mathcal{L}\rho(t), \tag{5b}$$

where $n_1 = c_1^\dagger c_1$ is the occupation number operator for dot 1 and the parameters $\mathcal{T}$ and $\mathcal{X}$ are given by $D = |\mathcal{T}|^2 = 2\pi e |T_{00}|^2 g_L g_R V/\hbar$ and $D' = |\mathcal{T} + \mathcal{X}|^2 = 2\pi e |T_{00} + \chi_{00}|^2 g_L g_R V/\hbar$. Here D and D' are the average electron tunneling rates through the PC barrier without and with the presence of the electron in dot 1, respectively, $eV = \mu_L - \mu_R$ is the external bias applied across the PC (μ_L and μ_R stand for the chemical potentials in the left and right reservoirs, respectively), T_{00} and χ_{00} are energy-independent tunneling amplitudes near the average chemical potential, and g_L and g_R are the energy-independent density of states for the left and right reservoirs. In Eq. (5a), the superoperator[39,48,42] $\mathcal{D}$ is defined as

$$\mathcal{D}[B]\rho = \mathcal{J}[B]\rho - \mathcal{A}[B]\rho, \tag{6}$$

where

$$\mathcal{J}[B]\rho = B\rho B^\dagger, \tag{7}$$

$$\mathcal{A}[B]\rho = (B^\dagger B\rho + \rho B^\dagger B)/2. \tag{8}$$

Finally, Eq. (5b) defines the Liouvillian operator $\mathcal{L}$.

Evaluating the density matrix operator in the logical qubit charge states, $|a\rangle$ and $|b\rangle$ (i.e., perfect localization state of the charge in dot 1 and dot 2, respectively), as in Ref. 17, we obtain

$$\dot{\rho}_{aa}(t) = i\Omega[\rho_{ab}(t) - \rho_{ba}(t)], \tag{9a}$$

$$\dot{\rho}_{ab}(t) = i\mathcal{E}\rho_{ab}(t) + i\Omega[\rho_{aa}(t) - \rho_{bb}(t)] - (|\mathcal{X}|^2/2)\rho_{ab}(t) + i\,\mathrm{Im}(\mathcal{T}^*\mathcal{X})\rho_{ab}(t), \tag{9b}$$

where $\hbar\mathcal{E} = \hbar(\omega_2 - \omega_1)$ is the energy mismatch between the two dots, $\Gamma_d = |\mathcal{X}|^2/2$ is the decoherence rate, and $\rho_{ij}(t) = \langle i|\rho(t)|j\rangle$. The relative phase between the two complex tunneling amplitudes ($\mathcal{T}$ and $\mathcal{X}$) [the last term in Eq. (9b)], cause an effective shift in the energy mismatch in the unconditional dynamics. Physically, the presence of the electron in dot 1 (state $|a\rangle$) raises the effective tunneling barrier of the PC due to electrostatic repulsion. As a consequence, the effective tunneling amplitude becomes lower, i.e., $D' = |\mathcal{T} + \mathcal{X}|^2 < D = |\mathcal{T}|^2$. This sets a condition on the relative phase θ between $\mathcal{X}$ and $\mathcal{T}$: $\cos\theta < -|\mathcal{X}|/(2|\mathcal{T}|)$.

III. CONDITIONAL MASTER EQUATION FOR INEFFICIENT MEASUREMENT

Equation (5) describes the time evolution of reduced density matrix when all the measurement results are ignored, or averaged over. To make contact with a single realization of the measurement records and study the stochastic evolution of the quantum state, conditioned on a particular measurement realization, the conditional master equation should be employed. The conditional master equations for a perfect detector in the quantum-jump and quantum diffusive cases have been derived in Refs. 25 and 26. In this paper, to take account the effect of the inefficiency in the measurements, which arises when the detector sometimes misses detection, we write first for the quantum-jump case that

$$[dN_c(t)]^2 = dN_c(t), \tag{10a}$$

$$E[dN_c(t)] = \zeta\,\mathrm{Tr}[\tilde{\rho}_{1c}(t+dt)] = \zeta[D + (D' - D)\langle n_1\rangle_c(t)]dt. \tag{10b}$$

Here the subscript c indicates that the quantity to which it is attached is conditioned on previous measurement results, the occurrences (detection records) of the electrons tunneling through the PC barrier in the past. In Eq. (10), $dN_c(t)$ is a stochastic point process which represents the number (either zero or one) of tunneling events seen in an infinitesimal time dt, $\langle n_1\rangle_c(t) = \mathrm{Tr}[n_1\rho_c(t)]$, $E[Y]$ denotes an ensemble average of a classical stochastic process Y, and

$$\tilde{\rho}_{1c}(t+dt) = \mathcal{J}[\mathcal{T} + \mathcal{X} n_1]\rho_c(t)dt \tag{11}$$

is the unnormalized density matrix[26] given the result of an electron tunneling through the PC barrier at the end of the time interval $[t, t+dt)$. The factor $\zeta \leqslant 1$ represents the fraction of detections which are actually registered by the PC detector. The value $\zeta = 1$ then corresponds to a perfect detector or efficient measurement. By using the fact that current through the PC is $i(t) = e\,dN(t)/dt$, Eq. (10b) with $\zeta = 1$ states that the average current is eD when dot 1 is empty, and is eD' when dot 1 is occupied. In Ref. 25 the case of inefficient measurements is discussed in terms of insufficiently small readout period. In other words, the bandwidth of the measurement device is not large enough to resolve and record every electron tunneling through the PC barrier.

By following the similar derivation as in Ref. 26, the stochastic quantum-jump master equation of the density matrix operator, conditioned on the observed event in the case of inefficient measurement in time dt can be obtained:

$$d\rho_c(t)=dN_c(t)\left[\frac{\mathcal{J}[\mathcal{T}+\mathcal{X}n_1]}{\mathcal{P}_{1c}(t)}-1\right]\rho_c(t)+dt\Big\{-\mathcal{A}[\mathcal{T}+\mathcal{X}n_1]\rho_c(t)+(1-\zeta)\mathcal{J}[\mathcal{T}+\mathcal{X}n_1]\rho_c(t)+\zeta\mathcal{P}_{1c}(t)\rho_c(t)-\frac{i}{\hbar}[\mathcal{H}_{\rm CQD},\rho_c(t)]\Big\}, \tag{12}$$

where

$$\mathcal{P}_{1c}(t)=D+(D'-D)\langle n_1\rangle_c(t). \tag{13}$$

In the quantum-jump case, in which individual electron tunneling current events can be distinguished, the qubit state [see Eq. (12)] undergoes a finite evolution (a *quantum jump*) when there is a detection result $[dN_c(t)=1]$ at randomly determined times (conditionally Poisson distributed).

The extension to the case of quantum diffusion can be carried out similarly as in Ref. 26. In this case, the electron counts or accumulated electron number in time δt is considered as a continuous diffusive variable satisfying a Gaussian white noise distribution[26,48]

$$\delta N(t)=\{\zeta|\mathcal{T}|^2[1+2\epsilon\cos\theta\langle n_1\rangle_c(t)]+\sqrt{\zeta}|\mathcal{T}|\xi(t)\}\delta t, \tag{14}$$

where $\epsilon=(|\mathcal{X}|/|\mathcal{T}|)\ll 1$, θ is the relative phase between $\mathcal{X}$ and $\mathcal{T}$, and $\xi(t)$ is a Gaussian white noise characterized by

$$E[\xi(t)]=0,\quad E[\xi(t)\xi(t')]=\delta(t-t'). \tag{15}$$

Here E denotes an ensemble average. In obtaining Eq. (14), we have assumed that $2|\mathcal{T}||\mathcal{X}|\cos\theta\gg|\mathcal{X}|^2$. Hence, for the quantum-diffusive equations obtained later, we should regard, to the order of magnitude, that $|\cos\theta|\sim O(1)\gg\epsilon=(|\mathcal{X}|/|\mathcal{T}|)$ and $|\sin\theta|\sim O(\epsilon)\ll 1$. The quantum-diffusive conditional master equation for the case of inefficient measurements can be found as

$$\dot\rho_c(t)=-\frac{i}{\hbar}[\mathcal{H}_{\rm CQD},\rho_c(t)]+\mathcal{D}[\mathcal{T}+\mathcal{X}n_1]\rho_c(t)+\xi(t)\frac{\sqrt{\zeta}}{|\mathcal{T}|}[\mathcal{T}^*\mathcal{X}n_1\rho_c(t)+\mathcal{X}^*\mathcal{T}\rho_c(t)n_1-2\,\mathrm{Re}(\mathcal{T}^*\mathcal{X})\langle n_1\rangle_c(t)\rho_c(t)]. \tag{16}$$

In arriving at Eq. (16), we have used the stochastic Itô calculus[49,50] for the definition of derivative as $\dot\rho(t)=\lim_{dt\to 0}[\rho(t+dt)-\rho(t)]/dt$. The conditional equations (12) and (16), under similar assumptions and approximations as in Ref. 26 but taking into account the effect of inefficient measurement, are the main results in this paper. We will analyze the qubit dynamics in detail in Sec. IV using these equations in terms of Bloch sphere variables [see Eqs. (20) and (21)]. In particular, the effect of inefficient measurements will be discussed in Sec. IV D. It is easy to see that the ensemble average evolution of Eq. (16) reproduces the unconditional master equation (5a) by simply eliminating the white noise term using Eq. (15). Similarly, averaging Eq. (12) over the observed stochastic process, by setting $E[dN_c(t)]$ equal to its expected value Eq. (10b), gives the unconditional, deterministic master equation (5a). It is also easy to verify that for zero efficiency $\zeta=0$ [i.e., also $dN_c(t)=0$], the conditional equations (12) and (16), reduce to the unconditional one (5a). That is, the effect of averaging over all possible measurement records is equivalent to the effect of completely ignoring the detection records or the effect of no detection results being available.

To make the quantum-diffusive, conditional stochastic master equation (16) more transparent, we evaluate Eq. (16) in the charge state basis as for Eq. (9) and obtain

$$\dot\rho_{aa}(t)=i\Omega[\rho_{ab}(t)-\rho_{ba}(t)]+\sqrt{8\zeta\Gamma_d}\cos\theta\rho_{aa}(t)\rho_{bb}(t)\xi(t), \tag{17a}$$

$$\dot\rho_{ab}(t)=i(\mathcal{E}+|\mathcal{T}||\mathcal{X}|\sin\theta)\rho_{ab}(t)+i\Omega[\rho_{aa}(t)-\rho_{bb}(t)]-\Gamma_d\rho_{ab}(t)+\sqrt{2\zeta\Gamma_d}\{\cos\theta[\rho_{bb}(t)-\rho_{aa}(t)]+i\sin\theta\}\rho_{ab}(t)\xi(t), \tag{17b}$$

where we have set $|\mathcal{X}|=\sqrt{2\Gamma_d}$. Again, either by taking ensemble average or for zero efficiency $\zeta=0$, Eq. (17) reduces to Eq. (9).

IV. CONDITIONAL DYNAMICS UNDER CONTINUOUS MEASUREMENTS

As in Ref. 26, we represent the qubit density matrix elements in terms of Bloch sphere variables in the charge state basis as

$$\rho(t)=[I+x(t)\sigma_x+y(t)\sigma_y+z(t)\sigma_z]/2, \tag{18}$$

where σ_i satisfies the properties of Pauli matrices. In this representation, the variable $z(t)$ represents the population difference between the two dots. Especially, $z(t)=1$ and $z(t)=-1$ indicate that the electron is localized in dot 2 and dot 1, respectively. The value $z(t)=0$ corresponds to an equal probability for the electron to be in each dot. Generally the product of the off-diagonal elements of $\rho(t)$ is smaller than the product of the diagonal elements, leading to the relation $x^2(t)+y^2(t)+z^2(t)\leq 1$. When $\rho(t)$ is represented by a pure state, the equal sign holds. In this case, the system state can be characterized by a point (x,y,z) on the Bloch unit sphere.

The master equations written as a set of coupled stochastic differential equations in terms of the Bloch sphere variables in Ref. 26 are under the assumptions of real tunneling amplitudes and perfect (efficient) measurements. Here we include the effect of inefficient measurement and the influence of the relative phase between the two tunneling amplitudes into the coupled equations. The unconditional master equation (5a) is equivalent to the following equations:

$$\frac{dx(t)}{dt}=-(\mathcal{E}+|\mathcal{T}||\mathcal{X}|\sin\theta)y(t)-\Gamma_d x(t), \tag{19a}$$

$$\frac{dy(t)}{dt}=(\mathcal{E}+|\mathcal{T}||\mathcal{X}|\sin\theta)x(t)-2\Omega z(t)-\Gamma_d y(t), \tag{19b}$$

$$\frac{dz(t)}{dt}=2\Omega y(t). \tag{19c}$$

We find that the quantum-diffusive, conditional master equation (16) can be written as

$$\frac{dx_c(t)}{dt}=-(\mathcal{E}+|\mathcal{T}||\mathcal{X}|\sin\theta)y_c(t)-\Gamma_d x_c(t)+\sqrt{2\zeta\Gamma_d}[-\sin\theta y_c(t)+\cos\theta z_c(t)x_c(t)]\xi(t), \tag{20a}$$

$$\frac{dy_c(t)}{dt}=(\mathcal{E}+|\mathcal{T}||\mathcal{X}|\sin\theta)x_c(t)-2\Omega z_c(t)-\Gamma_d y_c(t)+\sqrt{2\zeta\Gamma_d}[\sin\theta x_c(t)+\cos\theta z_c(t)y_c(t)]\xi(t), \tag{20b}$$

$$\frac{dz_c(t)}{dt}=2\Omega y_c(t)-\sqrt{2\zeta\Gamma_d}\cos\theta[1-z_c^2(t)]\xi(t). \tag{20c}$$

For the quantum-jump, conditional master equation (12), we obtain

$$dx_c(t)=dt\left(-[\mathcal{E}+(1-\zeta)|\mathcal{T}||\mathcal{X}|\sin\theta]y_c(t)-(1-\zeta)\Gamma_d x_c(t)-\frac{\zeta(D'-D)}{2}z_c(t)x_c(t)\right)-dN_c(t)\times\left(\frac{2|\mathcal{T}||\mathcal{X}|\sin\theta y_c(t)+[2\Gamma_d-(D'-D)z_c(t)]x_c(t)}{2D+(D'-D)[1-z_c(t)]}\right), \tag{21a}$$

$$dy_c(t)=dt\left([\mathcal{E}+(1-\zeta)|\mathcal{T}||\mathcal{X}|\sin\theta]x_c(t)-(1-\zeta)\Gamma_d y_c(t)-2\Omega z_c(t)-\frac{\zeta(D'-D)}{2}z_c(t)y_c(t)\right)-dN_c(t)\times\left(\frac{-2|\mathcal{T}||\mathcal{X}|\sin\theta x_c(t)+[2\Gamma_d-(D'-D)z_c(t)]y_c(t)}{2D+(D'-D)[1-z_c(t)]}\right), \tag{21b}$$

$$dz_c(t)=dt\left(2\Omega y_c(t)+\frac{\zeta(D'-D)}{2}[1-z_c^2(t)]\right)-dN_c(t)\left(\frac{(D'-D)[1-z_c^2(t)]}{2D+(D'-D)[1-z_c(t)]}\right). \tag{21c}$$

As expected, Eq. (20) averaged over the white noise reduces to Eq. (19), provided that $E[x_c(t)]=x(t)$ as well as similar replacements are performed for $y_c(t)$ and $z_c(t)$. Similarly, by using Eq. (10b), the ensemble average of Eq. (21) reduces to the unconditional equation (19). One can also observe that for zero efficiency $\zeta=0$, the conditional equations (21) and (20), reduce to the unconditional equation (19) as well. Next we analyze the qubit dynamics in detail and present the numerical simulations for the time evolution using Eqs. (20) and (21). Part of the results in Sec. IV A have been reported in Ref. 51.

A. From quantum jumps to quantum diffusion

Figure 2(a) shows the unconditional (ensemble average) time evolution of the population difference $z(t)$ with the initial qubit state being in state $|a\rangle$, i.e., dot 1 is occupied. The unconditional population difference $z(t)$, rises from -1, undergoing some oscillations, and then tends towards zero, a steady (maximally mixed) state. On the other hand, the conditional time evolution, conditioned on one possible individual realization of the sequence of measurement results, behaves quite differently. We consider first the situation, where $D'=|\mathcal{T}+\mathcal{X}|^2=0$, discussed in Ref. 18. In this case, due to the electrostatic repulsion generated by the electron, the PC is blocked (no electron is transmitted) when dot 1 is occupied. As a consequence, whenever there is a detection of an electron tunneling through the PC barrier, the qubit state is collapsed into state $|b\rangle$, i.e., dot 2 is occupied. The quantum-jump conditional evolution shown in Fig. 2(b) [using the same parameters and initial condition as in Fig. 2(a)] is rather obviously different from the unconditional one in Fig. 2(a). The conditional time evolution is not smooth, but exhibits jumps, and it does not tend towards a steady state. One can see that initially the system starts to undergo an oscillation. As the population difference $z_c(t)$ changes in time, the probability for an electron tunneling through the PC barrier increases. This oscillation is then interrupted by the detection of an electron tunneling through the PC barrier, which bring $z_c(t)$ to the value 1, i.e., the qubit state is collapsed into state $|b\rangle$. Then the whole process starts again. The randomly distributed moments of detections, $dN_c(t)$, corresponding to the quantum jumps in Fig. 2(b) is illustrated in Fig. 2(c). Although little similarity can be observed between the time evolution in Figs. 2(a) and 2(b), averaging over many individual realizations shown in Fig. 2(b) leads to a closer and closer approximation of the ensemble average in Fig. 2(a).

Next we illustrate how the transition from the quantum-jump picture to the quantum-diffusive picture takes place. In

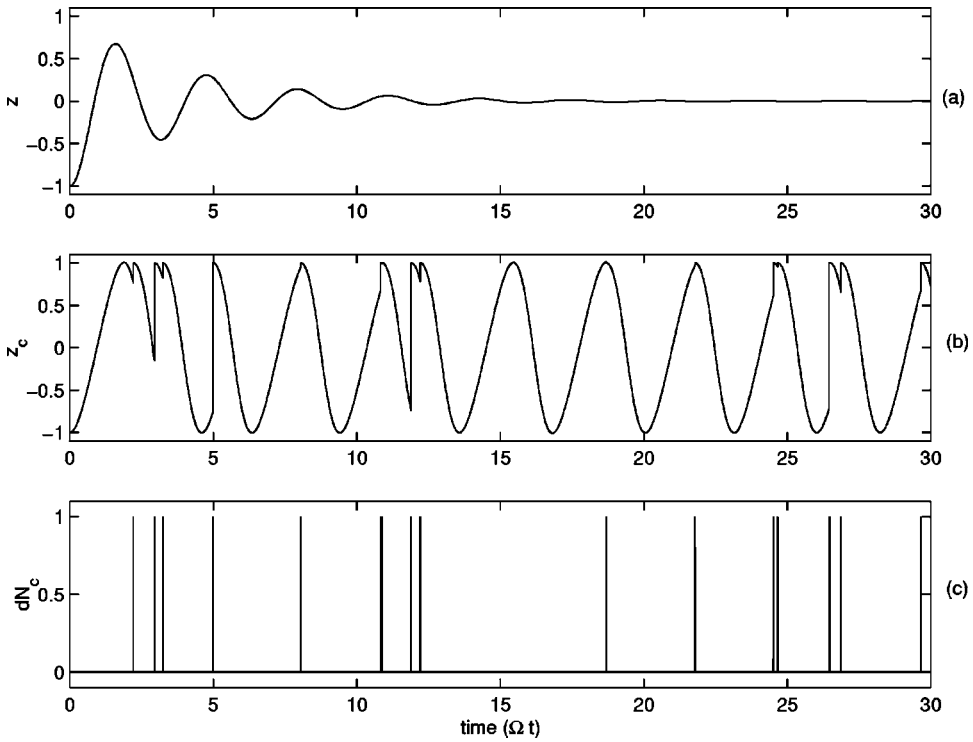

FIG. 2. Illustration for different behaviors between unconditional and conditional evolutions. The initial qubit state is $|a\rangle$. The parameters are $\zeta=1$, $\mathcal{E}=0$, $\theta=\pi$, $|\mathcal{T}|^2=|\mathcal{X}|^2=\Omega$, and time is in units of Ω^{-1}. (a) Unconditional, ensemble-averaged time evolution of $z(t)$, which exhibits some oscillation and then approaches a zero steady state value. (b) Conditional evolution of $z_c(t)$. The qubit starts an oscillation, which is then interrupted by a quantum jump [corresponding to a detection of an electron passing through the PC barrier in (c)]. After the jump, the qubit state is reset to $|b\rangle$ and a new oscillation starts. (c) Randomly distributed moments of detections, which correspond to the quantum jumps in (b).

Ref. 26 and Sec. III, we have seen that the quantum-diffusive equations can be obtained from the quantum-jump description under the assumption of $|\mathcal{T}|\gg|\mathcal{X}|$. In Figs. 3(a)–3(d) we plot conditional, quantum-jump evolution of $z_c(t)$ and the corresponding moments of detections $dN_c(t)$, with different ($|\mathcal{T}|/|\mathcal{X}|$) ratios. Each jump (discontinuity) in the $z_c(t)$ curves corresponds to the detection of an electron through the PC barrier. One can clearly observes that with increasing ($|\mathcal{T}|/|\mathcal{X}|$) ratio, the number of jumps increases. The amplitudes of the jumps of $z_c(t)$, however, decreases from $D'=0$ with the certainty of the qubit being in state $|b\rangle$ to the case of $(D-D')\ll(D+D')$ with a smaller probability of finding the qubit in state $|b\rangle$. Nevertheless, the population difference $z_c(t)$ always jumps up since $D=|\mathcal{T}|^2>D'=|\mathcal{T}+\mathcal{X}|^2$. In other words, whenever there is a detection of an electron passing through PC, dot 2 is more likely occu-

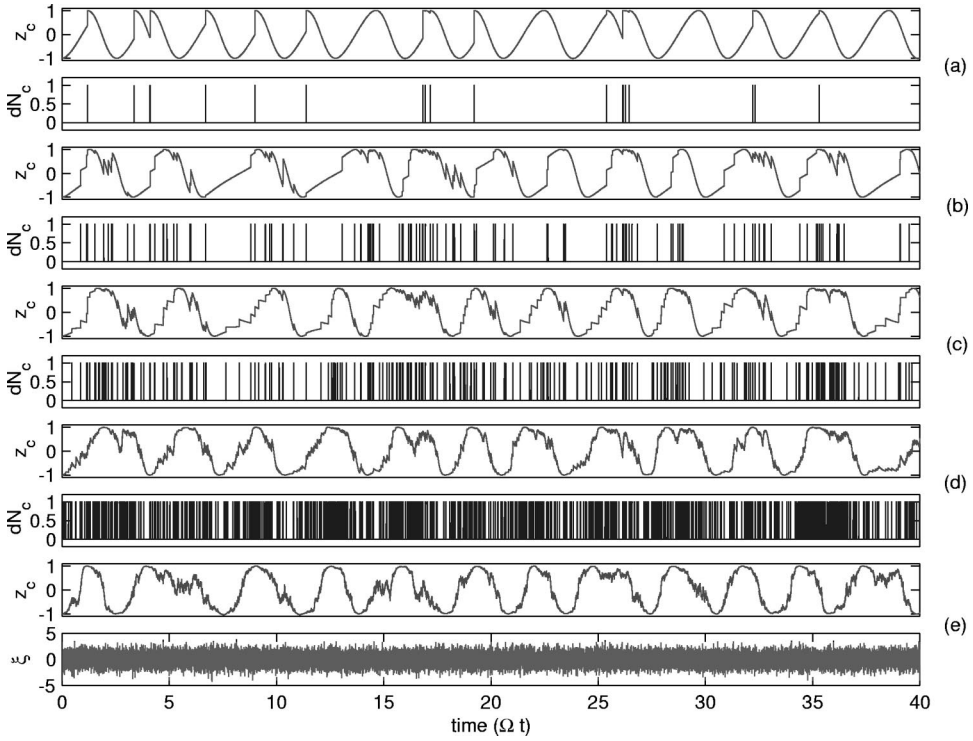

FIG. 3. Transition from quantum jumps to quantum diffusion. The initial qubit state is $|a\rangle$. The parameters are $\zeta=1$, $\mathcal{E}=0$, $\theta=\pi$, $|\mathcal{X}|^2=\Omega$, and time is in units of Ω^{-1}. (a)–(d) are the quantum-jump, conditional evolutions of $z_c(t)$, and corresponding detection moments with different $|\mathcal{T}|/|\mathcal{X}|$ ratios: (a) 1, (b) 2, (c) 3, (d) 5. With increasing $|\mathcal{T}|/|\mathcal{X}|$ ratio, jumps become more frequent but smaller in amplitude. (e) Represents the conditional evolutions of $z_c(t)$ in the quantum diffusive limit. The variable $\xi(t)$, appearing in the expression of current through PC in quantum-diffusive limit, is a Gaussian white noise with zero mean and unit variance.

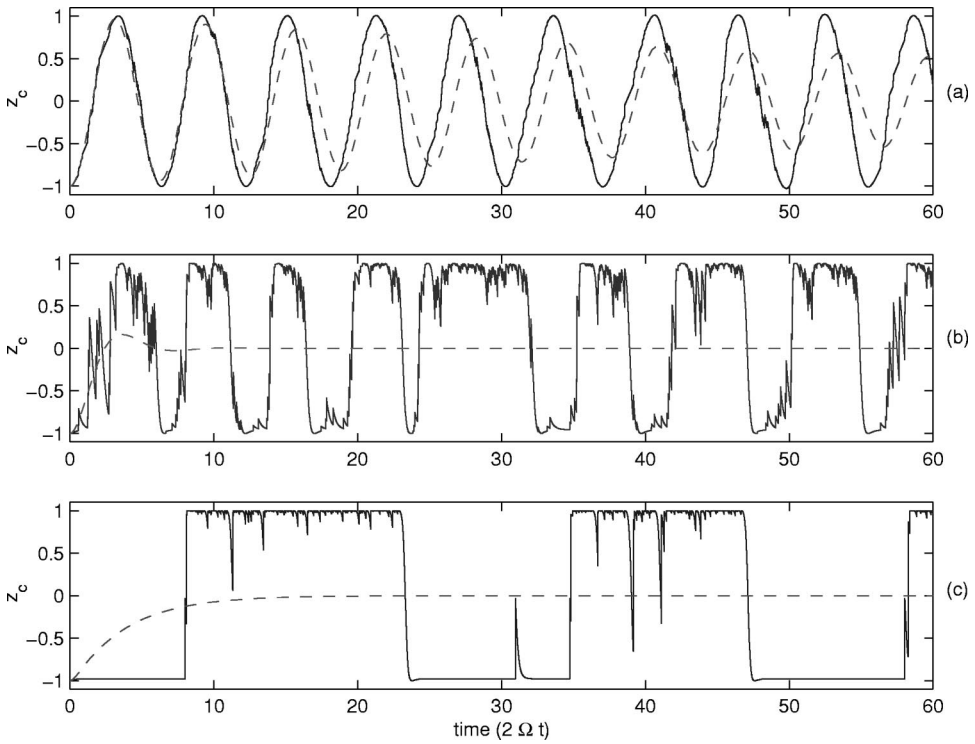

FIG. 4. Illustration of the quantum Zeno effect. Both conditional (in solid line) and unconditional (in dashed line) evolutions of the population difference for different ratios of (a) $(\Gamma_d/\Omega)=0.04$, (b) 2, (c) 8, are shown. The initial qubit state is $|a\rangle$. The other parameters are $\zeta=1$, $\mathcal{E}=0$, $\theta=\pi$, $|\mathcal{T}|^2=20\Omega$, and time is in units of $(2\Omega)^{-1}$. Increasing (Γ_d/Ω) ratio increases the period of coherent oscillations between the qubit states, while the time of a transition (switching time) decreases.

pied than dot 1. The case for quantum diffusion using Eq. (20) is plotted in Fig. 3(e). In this case, very small jumps occur very frequently. We can see that the behavior of $z_c(t)$ for $|\mathcal{T}|=5|\mathcal{X}|$ in the quantum-jump case shown in Fig. 3(d) is already very close to that of quantum diffusion shown in Fig. 3(e). To minimize the number of controllable variables, the same randomness is applied to produce the quantum-jump, conditional evolutions in Figs. 3(a)–3(d). This, however, does not mean that they would have had the same detection output, $dN_c(t)$. The number of tunneling events in time dt, $dN_c(t)$, does not depend on the randomness alone. It also depends on $|\mathcal{T}|$, $|\mathcal{X}|$, and θ, and has to satisfy Eq. (10b) in a self-consistent manner. In fact, it both conditions and is conditioned by the conditional qubit density matrix. Note that the unconditional evolution does not depend on the parameter $|\mathcal{T}|$ when $\theta=\pi$ [see Eq. (19)]. This implies that depending on the actual measured detection events, different measurement schemes (measurement devices with different tunneling barriers or different values of $|\mathcal{T}|$ when $\theta=\pi$) give different conditional quantum evolutions. But they would have the same ensemble average property if other parameters and the initial condition are the same. Hence, averaging over all possible realizations, for each measurement scheme in Fig. 3, will lead to the same ensemble average behavior shown in Fig. 2(a).

B. Quantum Zeno effect

The quantum Zeno effect can be naturally described by the conditional dynamics. The case for quantum diffusion has been discussed in Refs. 19 and 21. Here, for completeness, we discuss the quantum-jump case. The quantum Zeno effect states that repeated observations of the system slow down transitions between quantum states due to the collapse of the wave function into the observed state. Alternatively, the interaction with one measurement apparatus destroys the quantum coherence (oscillations) between $|a\rangle$ and $|b\rangle$ at a rate that is much faster than the tunneling rate Ω. For fixed Ω, $|\mathcal{T}|$, and θ, by increasing the interaction with the PC detector $|\mathcal{X}|=\sqrt{2\Gamma_d}$, we increase the number and amplitude of jumps and hence the probability of the wave function being collapsed to the localized state. The time evolutions of the population difference $z_c(t)$ for different ratios of (Γ_d/Ω) are shown in Fig. 4. Here, the initial qubit state is $|a\rangle$, and other parameters are $\zeta=1,\mathcal{E}=0,\theta=\pi,|\mathcal{T}|^2=10\Omega$. We can observe that the period of coherent oscillations between the two qubit states increases with increasing (Γ_d/Ω), while the time of a transition (switching time) decreases. In the limit of vanishing Ω, a transition from one qubit state to the other state takes a time (switching time) of order of localization time,[26] $1/\gamma_{\rm loc}^{\rm jump}=(D+D')/[\Gamma_d(\sqrt{D}+\sqrt{D'})^2]$. In the parameter regime of Fig. 4(c) $(\Gamma_d/\Omega=8)$, this time is still much smaller than the average time between state-changing transitions (period of oscillations) due to Ω, i.e., the mixing time,[26] $1/\gamma_{\rm mix}=\Gamma_d/(4\Omega^2)$. Hence, we can already see from Fig. 4(c) for $\Gamma_d/\Omega=8$ that very frequent repeated measurements would tend to localize the system.

The ensemble average behavior of $z(t)$ is also shown in dashed line in Fig. 4. If $\mathcal{E}=0$ and initially the electron is in dot 1, from the solution of Eq. (9), the probability $\rho_{aa}(t)=[1-z(t)]/2$ can be written as

$$\rho_{aa}(t)=\frac{1}{2}\left\{1+e^{-\Gamma_d t/2}\left[\cosh\left(\frac{\Omega_\Gamma}{2}t\right)+\frac{\Gamma_d}{\Omega_\Gamma}\sinh\left(\frac{\Omega_\Gamma}{2}t\right)\right]\right\}, \tag{22}$$

where $\Omega_\Gamma=\sqrt{\Gamma_d^2-(4\Omega)^2}$. In the Appendix, the stationary noise power spectrum of the current fluctuations through the

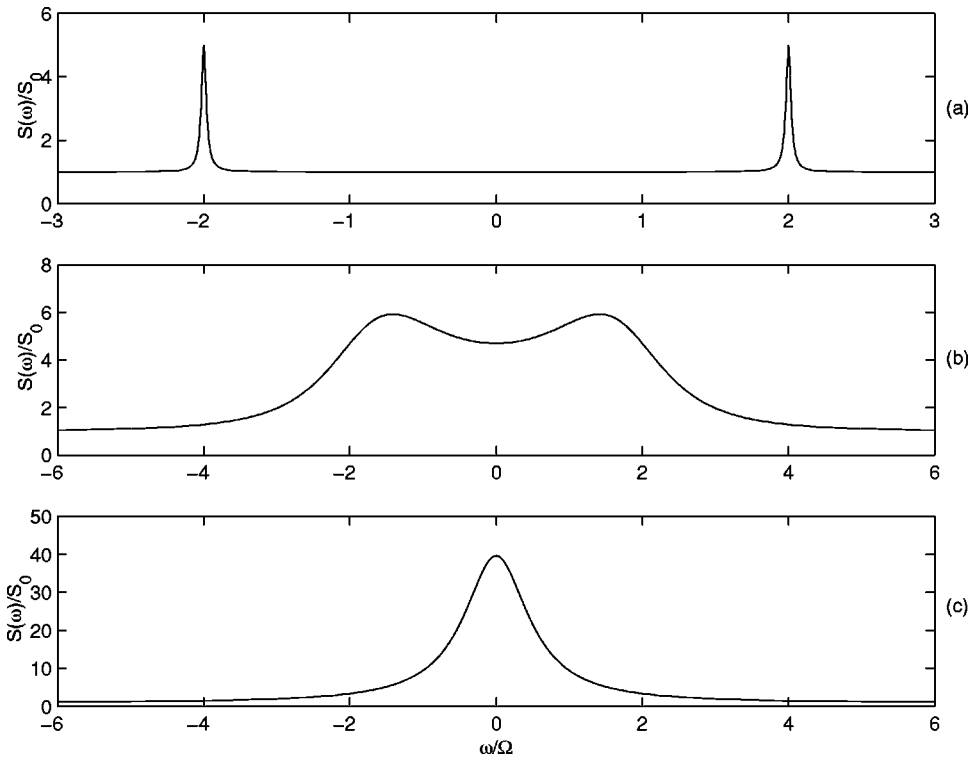

FIG. 5. A plot of the noise power spectrum of the current, normalized by the shot noise level for different ratios of (a) $(\Gamma_d/\Omega)=0.04$, (b) 2, (c) 8. All the parameters are the same as the corresponding ones in Fig. 4. For small (Γ_d/Ω) ratio, two sharp peaks appear in the noise power spectrum, as shown in (a). In (b), a double peak structure is still visible, indicating that coherent tunneling between the two qubit states still exists. In the classical, incoherent regime $\Gamma_d \geqslant 4\Omega$, only one single peak appears, as shown in (c).

PC barrier is calculated for the case of $\mathcal{E}=0$ and the result can be written as:[21]

$$S(\omega)=S_0+\frac{4\Omega^2(\Delta i)^2\Gamma_d}{(\omega^2-4\Omega^2)^2+\Gamma_d^2\omega^2}. \tag{23}$$

where $S_0=2ei_\infty=e^2\zeta(D'+D)$ represents the shot noise, $i_\infty=e\zeta(D'+D)/2$ is the steady-state current and $\Delta i=e\zeta(D-D')$ represents the difference between the two average currents. For $\Gamma_d<4\Omega$, $\rho_{aa}(t)$ shows the damped oscillatory behavior in the immediate time regime [see dashed line in Figs. 4(a) and 4(b)]. In this case, the spectrum has a double peak structure, indicating that coherent tunneling is taking place between the two qubit states. This is illustrated in Figs. 5(a) and 5(b). When $\Gamma_d \geqslant 4\Omega$, $\rho_{aa}(t)$ does not oscillate but decays in time purely exponentially, saturating at the probability 1/2 [see dashed line in Fig. 4(c)]. This corresponds to a classical, incoherent behavior. In this case, only a single peak, centering at $\omega=0$, appears in the noise spectrum, as illustrated in Fig. 5(c). The evolution of $z_c(t)$ in Fig. 4(c), is one of the possible conditional evolutions in this parameter regime $(\Gamma_d/\Omega=8)$. In this parameter regime $\Gamma_d \geqslant 4\Omega$, the conditional evolution $z_c(t)$ behaves very close to a probabilistic jumping or random telegraph process. After ensemble averaging over all possible realizations of such conditional evolutions, one would then obtain the classical, incoherent behavior.

C. Relative phase of the tunneling amplitudes

The relative phase between the two complex tunneling amplitudes produces effects on both conditional and unconditional dynamics of the qubit. In the following, we consider the case that $\zeta=1$ and $\mathcal{E}=0$. From Eq. (21), after each jump the imaginary part of the product $(\mathcal{T}^*\mathcal{X})$ seems to cause an additional rotation around the z axis in the Bloch sphere, but does not directly change the population probability $z_c(t)$ of the qubit. However, the actual conditional evolution of the Bloch sphere variables is complicated. It is stochastic and nonlinear, and depends on the relative phase of the tunneling amplitudes in a nontrivial way. Nevertheless, after ensemble average, the imaginary part of $(\mathcal{T}^*\mathcal{X})$ generates an effective shift in the energy mismatch of the qubit states [see Eq. (9)].

There are situations in which the effect of the relative phase of the tunneling amplitudes can be easily seen. For $\zeta=1$ and $\mathcal{E}=0$, if the tunneling amplitudes are real, i.e., $\theta=\pi$, and the initial condition $x_c(0)=0$, then the time evolution of $x_c(t)$, from Eq. (21), does not change and remains at the value 0 at all times. But if $\theta\neq\pi$ or $\sin\theta\neq 0$, the conditional evolution of $x_c(t)$ behaves rather differently. It changes after the first detection (quantum jump) takes place. Figure 6 shows the evolutions of the Bloch variables $x_c(t), y_c(t), z_c(t)$ with the same initial condition (the qubit being in $|a\rangle$) and parameters but different relative phases: $\theta=\pi$ for (a)–(c) and $\theta=\cos^{-1}(|\mathcal{X}|/|\mathcal{T}|)$ for (d)–(f). We can clearly see quite different behaviors of $x_c(t)$ in these two cases. The asymmetry of the electron population in $z_c(t)$, due to effectively generated energy mismatch in the second case in Fig. 6(f), can be roughly observed. The effect of the relative phase is small in the case of quantum diffusion. As noted in Sec. III, in order for the quantum-diffusive equations to be valid, we should regard, to the order of magnitude, that $|\cos\theta|\sim O(1)$ and $|\sin\theta|\sim O(\epsilon)$. This implies that in this case $\theta\approx\pi$. Hence the effect of the relative phase is small and the conditional dynamics does not deviate much from the case that the tunneling amplitudes are assumed to be real.[19,21,25]

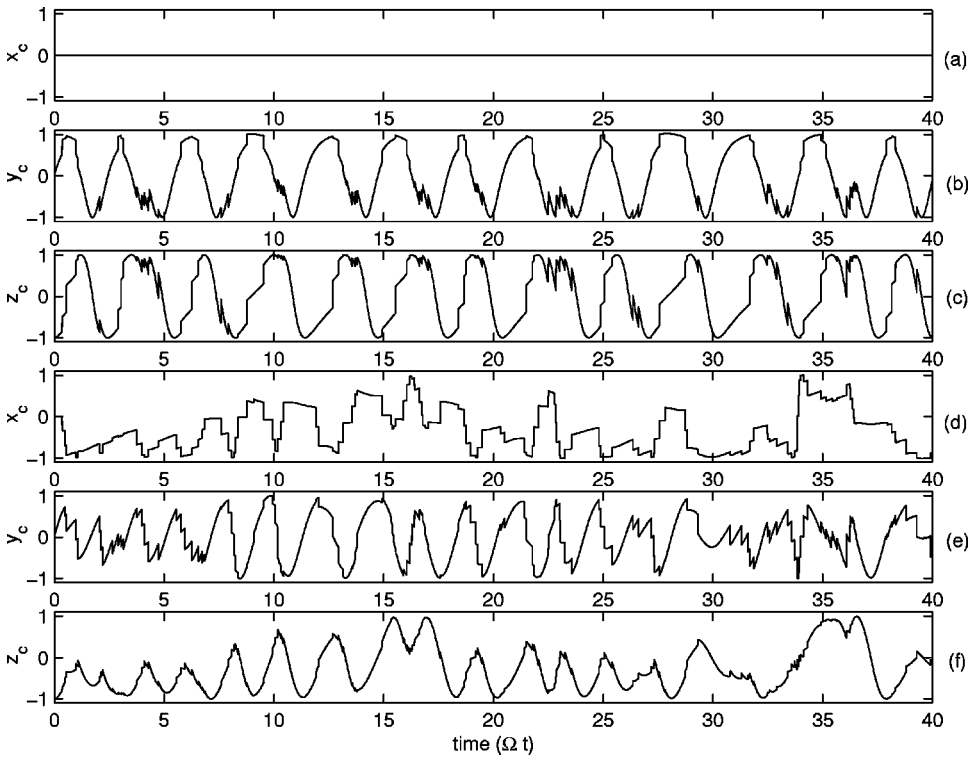

FIG. 6. Effect of relative phase on the qubit dynamics. The conditional evolutions of $x_c(t)$, $y_c(t)$, and $z_c(t)$ with the same initial condition (the qubit being in $|a\rangle$) and parameters ($\zeta=1$, $\mathcal{E}=0$, $\theta=\pi$, $|\mathcal{T}|^2=4|\mathcal{X}|^2=4\Omega$), but different relative phases are shown: (a)–(c) for $\theta=\pi$ and (d)–(f) for $\theta=\cos^{-1}(|\mathcal{X}|/|\mathcal{T}|)$. The relative phase causes quite different evolutions for $x_c(t)$.

D. Inefficient measurement and non-ideality

We have shown[26] that for $\zeta=1$, the conditional time evolution of the qubit can be described by a ket state vector satisfying the stochastic Schrödinger equation. It is then obvious that perfect detection or efficient measurement preserves state purity for a pure initial state. However, the inefficiency and nonideality of the detector spoils this picture. The decrease in our knowledge of the qubit state leads to partial decoherence for the qubit state. We next find the partial decoherece rate introduced in this way.

The stochastic differential equations in the form of Itô calculus[49,50] have the advantage that it is easy to see that the ensemble average of the conditional equations over the random process $\xi(t)$ leads to the unconditional equations. However, it is not a natural physical choice. For example, for $\zeta=1$, the term $-\Gamma_d\rho_{ab}(t)$ in Eq. (17b) does not really cause decoherence of the conditional qubit density matrix. It simply compensates the noise term due to the definition of derivative in Itô calculus. Hence, in this case the conditional evolution of $\rho_{ab}(t)$ does not really decrease in time exponentially. To find the partial decoherence rate generated by inefficiency $\zeta<1$, we transform Eq. (17b) into the form of Stratonovich calculus.[49,50] We then obtain for $\theta=\pi$:

$$\dot{\rho}_{ab}(t)=i\mathcal{E}\rho_{ab}(t)+i\Omega[\rho_{aa}(t)-\rho_{bb}(t)] -[\rho_{bb}(t)-\rho_{aa}(t)]\frac{\sqrt{2\Gamma_d}}{e|\mathcal{T}|}[i(t)-i_0]\rho_{ab}(t) -(1-\zeta)\Gamma_d\rho_{ab}(t), \tag{24}$$

where $i(t)-i_0=e|\mathcal{T}|\{\zeta\sqrt{2\Gamma_d}[1-2\rho_{aa}(t)]+\sqrt{\zeta}\xi(t)\}$. Here we have used the following relations: the conditional current $i(t)=e\,\delta N(t)/\delta t$ with $\delta N(t)$ given by Eq. (14) and the average current $i_0=e\zeta(D+D')/2$, where $D=|\mathcal{T}|^2$ and $D'=|\mathcal{T}|^2-2|\mathcal{T}||\mathcal{X}|$ in the quantum-diffusive limit. In this form, Eq. (24) elegantly shows how the qubit density matrix is conditioned on the measured current. We find that the last term in Eq. (24) is responsible for decoherence. In other words, the partial decoherence rate for an individual realization of inefficient measurements is $(1-\zeta)\Gamma_d$. For a perfect detector $\zeta=1$, this decoherence rate vanishes and the conditional $\rho_{ab}(t)$, as expected, does not decay exponentially in time. Similar conclusion could be drawn from Eq. (21) for the quantum-jump case. For $\theta=\pi$, the off-diagonal variables $x_c(t)$ and $y_c(t)$ seem to decrease in time with the rate $(1-\zeta)\Gamma_d$.

In Bloch sphere variable representation, we can use the quantity $P_c(t)=x_c^2(t)+y_c^2(t)+z_c^2(t)$ as a measure of the purity of the qubit state, or equivalently as a measure of how much information the conditional measurement record gives about the qubit state. If the conditional state of the qubit is a pure state then $P_c(t)=1$; if it is a maximally incoherent mixed state then $P_c(t)=0$. We plot in Fig. 7 the quantum-jump, conditional evolution of the purity $P_c(t)$ for different inefficiencies, $\zeta=1,0.6,0.2$ (in solid line), and 0 (in dotted line). Figure 7(a) is for an initial qubit state being in a pure state $|a\rangle$, while Fig. 7(b) is for a maximally mixed initial state. We can see from Fig. 7(a) that the purity $P_c(t)=1$ at all times for $\zeta=1$, while it hardly or not at all reaches 1 for almost all time for $\zeta<1$. This means that partial information about the changes of the qubit state is lost irretrievably in inefficient measurements. In addition, roughly speaking, the overall behavior of $P_c(t)$ decreases with decreasing ζ. This indicates that after being averaged over a long period of time, $\langle P_c(t)\rangle_t$ would also decrease with decreasing ζ. For

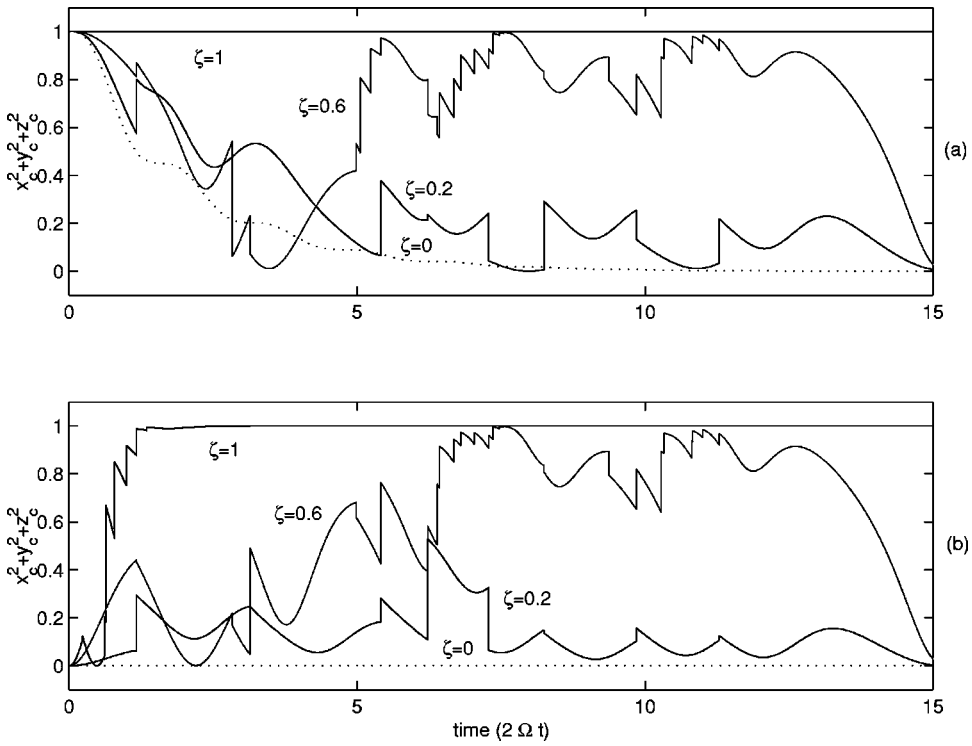

FIG. 7. Effect of inefficiency on the state purity. The quantum-jump, conditional evolution of the purity $P_c(t)$ for different inefficiencies, $\zeta=1,0.6,0.2$ (in solid line), and 0 (in dotted line) are plotted in (a) for an initial qubit state being in a pure state $|a\rangle$, (b) for a maximally mixed initial state. The other parameters are $\mathcal{E}=0$, $\theta=\pi$, $|\mathcal{T}|^2=4|\mathcal{X}|^2=4\Omega$. The purity-preserving conditional evolution for a pure initial state, and gradual purification for a nonpure initial state for $\zeta=1$ are illustrated. However, the complete purification of the qubit state cannot be achieved for $\zeta<1$.

$\zeta=0$, the evolution of $P(t)$ becomes smooth and tends toward the value zero (the maximally mixed steady state). For a nonpure initial state [see Fig. 7(b)], the qubit state is eventually collapsed towards a pure state and then remains in a pure state for $\zeta=1$. But the complete purification of the qubit state cannot be achieved for $\zeta<1$. As in Figs. 3(a)–3(d), the same randomness has been applied to generate the quantum-jump, conditional evolution in Figs. 7(a) and 7(b). Note that the only difference between evolution in Fig. 7(a) and the corresponding one in Fig. 7(b) is the different initial states. So when the qubit density matrix in Fig. 7(b) gradually evolves into the same state as in Fig. 7(a), the corresponding $P_c(t)$ in Fig. 7(b) would then follow the same evolution as in Fig. 7(a). This behavior can be observed in Fig. 7. The purity-preserving conditional evolution for a pure initial state, and gradual purification for a nonpure initial state for an ideal detector have been discussed in Refs. 19–21,24 in the quantum-diffusive limit.

The nonideality of the PC detector is modeled in Refs. 19–21,24 by another ideal detector ''in parallel'' to the original one but with inaccessible output. We can add, as in Refs. 19–21,24, an extra term, $-\gamma_d\rho_{ab}(t)$, to Eq. (24) to account for the ''nonideality'' of the detector. The ideal factor η introduced there[19–21,24] can be modified to take account of inefficient measurement discussed here. We find

$$\eta=1-\frac{\Gamma}{\Gamma_{\rm tot}}=\frac{\zeta\Gamma_d}{\Gamma_d+\gamma_d}, \tag{25}$$

where $\Gamma=(1-\zeta)\Gamma_d+\gamma_d$ and $\Gamma_{\rm tot}=\Gamma_d+\gamma_d$. For $\gamma_d=0$, we have $\eta=\zeta$. In Ref. 25, inefficient measurement is discussed in terms of insufficiently small readout period. As a result, the information about the tunneling times of the electrons passing through the PC barrier is partially lost.

V. CONCLUSION

We have obtained the quantum-jump and quantum-diffusive, conditional master equations, taking into account the effect of inefficient measurements $\zeta\leqslant 1$ under the weak system-environment coupling and Markovian approximations. These conditional master equations describe the random evolution of the measured qubit density matrix, which both conditions and is conditioned on, a particular realization of the measured current. If and only if detections are perfect (efficient measurement), i.e., $\zeta=1$, are the stochastic master equations for the conditioned density matrix operators (12) and (16), equivalent to the stochastic Schrödinger equations [Eqs. (35) and (41) of Ref. 26, respectively] for the conditioned states. If the detection is not perfect and some information about the system is *unrecoverable*, the evolution of the system can no longer be described by a pure state vector. For the extreme case of zero efficiency detection, the information (measurement results at the detector) carried away from the system to the reservoirs is (are) completely ignored, so that the stochastic master equations (12) and (16) after being averaged over all possible measurement records reduces to the unconditional, deterministic master equation (5a), leading to decoherence for the system.

We have used the derived conditional equations to analyze the conditional qubit dynamics in detail and illustrate the conditional evolution by numerical simulations. Specifically, the conditional qubit dynamics evolving from quantum jumps to quantum diffusion has been presented. Furthermore, we have described the quantum Zeno effect in terms of the quantum-jump conditional dynamics. We have calculated the stationary noise power spectrum of the current fluctuations through the PC barrier in terms of the quantum-jump formalism. We have also discussed the effect of inefficient

measurement and the influence of relative phase between the two tunneling amplitudes on the qubit dynamics.

ACKNOWLEDGMENTS

H.S.G. is grateful for useful discussions with A. N. Korotkov, G. Schön, D. Loss, Y. Hirayama, J. S. Tsai, and G. P. Berman. H.S.G. would like to thank H. B. Sun and H. M. Wiseman for their assistance and discussions in the early stage of this work.

APPENDIX: CALCULATION OF THE NOISE POWER SPECTRUM OF THE CURRENT FLUCTUATIONS

In this Appendix, we calculate the stationary noise power spectrum of the current fluctuations through the PC when there is the possibility of coherent tunneling between the two qubit states. Usually one can calculate this noise power spectrum using the unconditional, deterministic master equation approach, which gives only the average characteristics. We, however, calculate it through the stochastic formalism presented here. The fluctuations in the observed current, $i(t)$, are quantified by the two-time correlation function:

$$G(\tau)=E[i(t+\tau)i(t)]-E[i(t+\tau)]E[i(t)]. \tag{A1}$$

The noise power spectrum of the current is then given by

$$S(\omega)=2\int_{-\infty}^{\infty}d\tau\, G(\tau)e^{-i\omega\tau}. \tag{A2}$$

The ensemble expectation values of the two-time correlation function for the current in the case of quantum diffusion has been calculated in Ref. 21. Here we will present the quantum-jump case. The current in this case is given by $i(t)=e\,dN(t)/dt$. We will follow closely the calculation in the Appendix of Ref. 39 to calculate the two-time correlation function, $E[dN_c(t+\tau)dN(t)]$. First we consider the case when $\tau\gg dt>0$, where dt is the minimum time step considered. Since $dN(t)$ is a classical point process, it is either zero or one. As a result, $E[dN_c(t+\tau)dN(t)]$ is nonvanishing only if there is an electron-tunneling event inside each of these two infinitesimal time intervals, $[t,t+dt]$ and $[t+\tau,t+\tau+dt]$. Hence, we can write

$$E[dN_c(t+\tau)dN(t)]=\mathrm{Prob}[dN(t)=1]E[dN_c(t+\tau)|_{dN(t)=1}], \tag{A3}$$

where the subscript to the vertical line is the condition for which the subscript on $dN_c(t+\tau)$ exists. From Eqs. (10b) and (11), we have $\mathrm{Prob}[dN(t)=1]=\zeta\,\mathrm{Tr}[\tilde{\rho}_1(t+dt)]$ and $E[dN_c(t+\tau)|_{dN(t)=1}]=\zeta\,\mathrm{Tr}\{\mathcal{J}[\mathcal{T}+\mathcal{X}n_1]E[\rho_{1c}(t+\tau)|_{dN(t)=1}]\}$. Using the fact that $E[\rho_c(t)]=\rho(t)$ and Eqs. (5b) and (11), we can write

$$\begin{aligned}E[\rho_{1c}(t+\tau)|_{dN(t)=1}]&=e^{\mathcal{L}(\tau-dt)}\tilde{\rho}_1(t+dt)/\mathrm{Tr}[\tilde{\rho}_1(t+dt)]\\&=\zeta e^{\mathcal{L}(\tau-dt)}\{\mathcal{J}[\mathcal{T}+\mathcal{X}n_1]\rho(t)dt\}/\\&\quad\mathrm{Tr}[\tilde{\rho}_1(t+dt)].\end{aligned} \tag{A4}$$

Hence, to leading order in dt, we obtain for $\tau>0$:

$$\begin{aligned}E[dN_c(t+\tau)dN(t)]=\zeta^2dt^2\,\mathrm{Tr}[\mathcal{J}[\mathcal{T}+\mathcal{X}n_1]\\\times e^{\mathcal{L}\tau}\{\mathcal{J}[\mathcal{T}+\mathcal{X}n_1]\rho(t)\}].\end{aligned} \tag{A5}$$

For $\tau=0$, we have, from Eq. (10), that

$$E[dN(t)dN(t)]=E[dN(t)]=\zeta[D+(D'-D)\langle n_1\rangle(t)]dt. \tag{A6}$$

For short times, this term dominates and we may regard $dN(t)/dt$ as δ-correlated noise for a suitably defined δ function. Thus the current-current two-time correlation function for $\tau\geqslant 0$ can be written as

$$\begin{aligned}E[i(t+\tau)i(t)]&=E\left[\frac{dN_c(t+\tau)}{dt}\frac{dN(t)}{dt}\right]\\&=e^2\zeta\{D+(D'-D)\mathrm{Tr}[n_1\rho(t)]\}\\&\quad\times\delta(\tau)+\zeta^2\,\mathrm{Tr}[\mathcal{J}[\mathcal{T}+\mathcal{X}n_1]\\&\quad\times e^{\mathcal{L}\tau}\{\mathcal{J}[\mathcal{T}+\mathcal{X}n_1]\rho(t)\}].\end{aligned} \tag{A7}$$

In this form, we have related the ensemble averages of classical random variable to the quantum averages with respect to the qubit density matrix. The case $\tau\leqslant 0$ is covered by the fact that the current–current two-time correlation function or $G(\tau)$ is symmetric in τ, i.e., $G(\tau)=G(-\tau)$.

Next we calculate steady-state $G(\tau)$ and $S(\omega)$. We can simplify Eq. (A7) using the following identities for an arbitrary operator B: $\mathrm{Tr}[\mathcal{J}[n_1]B]\equiv\mathrm{Tr}[n_1B]$, $\mathrm{Tr}[e^{\mathcal{L}\tau}B]=\mathrm{Tr}[B]$, and $\mathrm{Tr}[Be^{\mathcal{L}\tau}\rho_\infty]=\mathrm{Tr}[B\rho_\infty]$, where the ∞ subscript indicates that the system is at the steady state and the steady-state density matrix ρ_∞ is a maximally mixed state. Hence we obtain the steady-state $G(\tau)$ for $\tau\geqslant 0$ as

$$\begin{aligned}G(\tau)=ei_\infty\delta(\tau)+e^2\zeta^2(D'-D)^2\\\times\{\mathrm{Tr}[n_1e^{\mathcal{L}\tau}[n_1\rho_\infty]-\mathrm{Tr}[n_1\rho_\infty]^2\},\end{aligned} \tag{A8}$$

where the steady-state average current $i_\infty=e\zeta(D+D')/2$. The first term in Eq. (A8) represents the shot noise component. It is easy to evaluate Eq. (A8) analytically for $\mathcal{E}=0$ case. The case for the asymmetric qubit, $\mathcal{E}\neq 0$, can be calculated numerically. Evaluating Eq. (A8) for $\mathcal{E}=0$, we find

$$G(\tau)=ei_\infty\delta(\tau)+\frac{(\Delta i)^2}{4}\left(\frac{\mu_+e^{\mu_-\tau}-\mu_-e^{\mu_+\tau}}{\mu_+-\mu_-}\right), \tag{A9}$$

where $\mu_\pm=-(\Gamma_d/2)\pm\sqrt{(\Gamma_d/2)^2-4\Omega^2}$, and we have represented $\Delta i=e\zeta(D-D')$ as the difference between the two average currents. After Fourier transform following from Eq. (A2), the power spectrum of the noise is then obtained as the expression of Eq. (23). Note that from Eq. (23), the noise spectrum at $\omega=2\Omega$ for $\theta=\pi$, i.e., real tunneling amplitudes, can be written as

$$\frac{S(2\Omega)-S_0}{S_0}=2\zeta\frac{(\sqrt{D}+\sqrt{D'})^2}{(D+D')}, \tag{A10}$$

where $S_0=2ei_\infty=e^2\zeta(D'+D)$ represents the shot noise. In obtaining Eq. (A10), we have used the relation $\Gamma_d=(\sqrt{D}-\sqrt{D'})^2/2$ for the case of real tunneling amplitudes. In the quantum-diffusive limit $|\mathcal{T}|\gg|\mathcal{X}|$ or $(D+D')\gg(D-D')$, this ratio $[S(2\Omega)-S_0]/S_0\to 4\zeta$, independent[21] of the values of Ω and Γ_d. These results for $\zeta=1$ and in the limit of quantum diffusion are consistent with those derived in Ref. 21 using both the unconditional master equation approach and conditional stochastic formalism with white noise current fluctuations for an ideal detector.

*Electronic mail: goan@physics.uq.edu.au

[1] D. P. DiVincenzo, Fortschr. Phys. **48**, 771 (2000).

[2] D. J. Wineland, C. Monroe, W. M. Itano, D. Leibfried, B. E. King, and D. M. Meekhof, J. Res. Natl. Inst. Stand. Technol. **103**, 259 (1998).

[3] B. E. Kane, Nature (London) **393**, 133 (1998); V. Privman, I. D. Vagner, and G. Kventsel, Phys. Lett. A **239**, 141 (1998).

[4] D. Loss and D. P. DiVincenzo, Phys. Rev. A **57**, 120 (1998); A. Imamoglu, D. D. Awschalom, G. Burkard, D. P. DiVincenzo, B. D. Loss, M. Sherwin, and A. Small, Phys. Rev. Lett. **83**, 4204 (1999).

[5] A. Shnirman, G. Schön, and Z. Hermon, Phys. Rev. Lett. **79**, 2371 (1997); D. V. Averin, Solid State Commun. **105**, 659 (1998).

[6] N. H. Bonadeo, J. Erland, D. Gammon, D. Park, D. S. Katzer, and D. G. Steel, Science **282**, 1473 (1998).

[7] T. Tanamoto, Phys. Rev. A **61**, 22 305 (2000).

[8] W. H. Zurek, Rev. Mod. Phys. (in press), quant-ph/0105127 (2001).

[9] D. W. Berry and H. M. Wiseman, Phys. Rev. Lett. **85**, 5098 (2000).

[10] A. Doherty, J. Doyle, H. Mabuchi, K. Jacobs, and S. Habib, ''Robust control in the quantum domain,'' Proceedings of the 39th IEEE Conference on Decision and Control, 2000, p. 949.

[11] C. H. Crouch, C. Livermore, R. M. Westervelt, K. L. Campman, and A. C. Gossard, Appl. Phys. Lett. **71**, 817 (1997).

[12] F. R. Waugh, M. J. Berry, D. J. Mar, R. M. Westervelt, K. L. Campman, and A. C. Gossard, Phys. Rev. Lett. **75**, 705 (1995).

[13] T. H. Oosterkamp, T. Fujisawa, W. G. van der Wiel, K. Ishibashi, R. V. Hijman, S. Tarucha, and L. P. Kouwenhoven, Nature (London) **395**, 873 (1998).

[14] T. Fujisawa, W. G. van der Wiel, and L. P. Kouwenhoven, Physica E (Amsterdam) **7**, 413 (2000).

[15] V. Bouchiat, D. Vion, P. Joyez, D. Esteve, and M. H. Devoret, Phys. Scr. **T76**, 165 (1998).

[16] Y. Nakamura, Yu. A. Pashkin, and J. S. Tsai, Nature (London) **398**, 786 (1999).

[17] S. A. Gurvitz, Phys. Rev. B **56**, 15 215 (1997).

[18] S. A. Gurvitz, quant-ph/9808058.

[19] A. N. Korotkov, Phys. Rev. B **60**, 5737 (1999).

[20] A. N. Korotkov, Physica B **280**, 412 (2000).

[21] A. N. Korotkov, Phys. Rev. B **63**, 85 312 (2001).

[22] Y. Makhlin, G. Schön, and A. Shnirman, cond-mat/9811029; Rev. Mod. Phys. **73**, 357 (2001).

[23] Y. Makhlin, G. Schön, and A. Shnirman, Phys. Rev. Lett. **85**, 4578 (2000).

[24] A. N. Korotkov, cond-mat/0008003.

[25] A. N. Korotkov, Phys. Rev. B **63**, 115403 (2001).

[26] H.-S. Goan, G. J. Milburn, H. M. Wiseman, and H. B. Sun, Phys. Rev. B **63**, 125326 (2001).

[27] I. L. Aleiner, N. S. Wingreen, and Y. Meir, Phys. Rev. Lett. **79**, 3740 (1997).

[28] Y. Levinson, Europhys. Lett. **39**, 299 (1997).

[29] L. Stodolsky, Phys. Lett. B **459**, 193 (1999).

[30] M. Büttiker and A. M. Martin, Phys. Rev. B **61**, 2737 (2000).

[31] G. Hackenbroich, B. Rosenow, and H. A. Weidenmüller, Phys. Rev. Lett. **81**, 5896 (1998).

[32] D. V. Averin, cond-mat/0004364; A. N. Korotkov and D. V. Averin, cond-mat/0002203.

[33] A. Shnirman and G. Schön, Phys. Rev. B **57**, 15 400 (1998).

[34] D. V. Averin, cond-mat/0008114; cond-mat/0010052.

[35] A. Maassen van den Brink, cond-mat/0009163.

[36] H. J. Carmichael, *An Open System Approach to Quantum Optics*, Lecture Notes in Physics (Springer, Berlin, 1993).

[37] J. Dalibard, Y. Castin, and K. Molmer, Phys. Rev. Lett. **68**, 580 (1992).

[38] N. Gisin and I. C. Percival, J. Phys. A **25**, 5677 (1992); **26**, 2233 (1993); **26**, 2245 (1993).

[39] H. M. Wiseman and G. J. Milburn, Phys. Rev. A **47**, 1652 (1993).

[40] M. J. Gagen, H. M. Wiseman, and G. J. Milburn, Phys. Rev. A **48**, 132 (1993).

[41] G. C. Hegerfeldt, Phys. Rev. A **47**, 449 (1993).

[42] H. M. Wiseman, Quantum Semiclassic. Opt. **8**, 205 (1996).

[43] C. Presilla, R. Onofrio, and U. Tambini, Ann. Phys. (Leipzig) **248**, 95 (1996).

[44] M. B. Mensky, Phys. Usp. **41**, 923 (1998).

[45] M. B. Plenio and P. L. Knight, Rev. Mod. Phys. **70**, 101 (1998).

[46] C. W. Gardiner and P. Zoller, *Quantum Noise*, 2nd ed. (Springer, Berlin, 2000).

[47] The finite-temperature unconditional master equation for the CQD system, taking into account the effect of thermal PC reservoirs under the weak system-environment coupling and Markovian approximations, is obtained in Ref. 26.

[48] H. M. Wiseman and G. J. Milburn, Phys. Rev. A **47**, 642 (1993).

[49] G. W. Gardiner, *Handbook of Stochastic Method* (Springer, Berlin, 1985).

[50] B. Øksendal, *Stochastic Differential Equations* (Springer, Berlin, 1992).

[51] H.-S. Goan and G. J. Milburn, *Proceedings of International Conference on Experimental Implementations of Quantum Computing, Sydney, Australia* (Rinton Press, Australia, 2001); cond-mat/0102058.